Molecular fluorescent pH-probes based on 8-hydroxyquinoline†

Stefan Kappaun,[a] Tanja Sović,[a] Franz Stelzer,[a] Alexander Pogantsch,[b] Egbert Zojer*[b,c] and Christian Slugovc*[a]

Received 19th January 2006, Accepted 15th February 2006
First published as an Advance Article on the web 14th March 2006
DOI: 10.1039/b600912c

Three 5,7-π-extended 8-benzyloxyquinolines, namely 5,7-diphenyl-, 5,7-bis(biphenyl-4-yl)- and 5,7-bis(4-dibenzothiophenyl)-8-benzyloxyquinoline were prepared and investigated as fluorescent pH-probes in nonaqueous solution. Absorption and photoluminescence spectra of the introduced compounds also including the starting material 8-benzyloxy-5,7-dibromoquinoline as well as their N-protonated counterparts were recorded and the results were rationalized by quantum-chemical calculations. A pronounced red shift of the emission occurred upon protonation of the non halogenated derivatives, while the dibromo-derivative is hardly emissive and is virtually not protonated under the conditions used. The diphenyl- and the bis(biphenyl)-derivative especially show promising photoluminescence quantum yields both in the parent and the protonated state making them candidates for the active component in pH sensing applications.

Introduction

The design and synthesis of fluorescent molecules with a sensing function is an area of intense research activity. A large number of chemosensors whose emission properties are modulated by external inputs have been described so far. Due to the high sensitivity of fluorescence spectroscopy, allowing the detection of very low concentrations of the analyte, in certain cases even down to individual molecules, fluorescent sensors and probes have been utilised in many areas such as medicine, industry and the environment.[1] While in many fluorescent chemosensors the interaction with the analyte only affects the emission intensity, a shift in the emission wavelength through the sensing process is preferable because of the possibility of signal rationing to increase the dynamic range and provide built-in correction for environmental effects.[2]

8-Hydroxyquinoline and its derivatives have found many applications in the fluorescent sensing of biological and environmentally important metal ions.[3] Nevertheless, just one study has hitherto been done dealing with the influence of acids and bases on 8-hydroxyquinoline and its derivatives.[4] Aside from this, 8-hydroxyquinolines have been used in electroluminescent complexes, most prominently tris(8-hydroxyquinoline)aluminium ([Alq_3]). [Alq_3] was introduced as an emitting material by Tang and VanSlyke. Since then these and analogous metal complexes have attracted a great interest in display applications.[5]

As a further advance in the development of fluorescent pH-probes, we report the synthesis, and photophysical as well as quantum-chemical characterization of modified 8-hydroxyquinoline derivatives starting from 5,7-dibromo-8-hydroxyquinoline. As it is well known that 8-hydroxyquinoline is weakly fluorescent because of the excited-state intramolecular proton transfer (ESIPT) of the proton of the *OH*-function to the *N* of the pyridine moiety,[3] our design is based on bonding alkyl chains to the *OH*-function of 8-hydroxyquinoline inhibiting this ESIPT pathway.[6]

Moreover, we pay particular attention to the effects of extending the π-system on emission behaviour. Two of the investigated molecules proved suitable as ratiometric pH probes in a non-aqueous environment making use of the protonation/deprotonation of the quinoline nitrogen atom.

Experimental

Materials and methods

Unless otherwise noted, materials were obtained from commercial sources (Aldrich, Fluka or Lancaster) and used without further purification. 8-Benzyloxy-5,7-dibromoquinoline (**2**), 8-benzyloxy-5,7-diphenylquinoline (**3**) and 8-hydroxy-5,7-diphenylquinoline (**6**) were prepared as reported in the literature.[7] ^{1}H-NMR spectra were recorded on a Varian INOVA 500 MHz spectrometer *versus* $SiMe_4$ as standard. $^{13}C\{^1H\}$-NMR spectra were recorded at 125 MHz. The solvent residual peak of $CDCl_3$ was used for referencing the NMR-spectra to 7.26 ppm and 77.16 ppm, respectively.[8] FT-IR spectra were obtained from films on NaCl windows with a Perkin Elmer Spectrum One and a DTGS-detector. UV/VIS absorption spectra were recorded on a Cary 50 Bio UV/Visible spectrophotometer, fluorescence spectra on a Perkin Elmer Luminescence Spectrometer LS50B. PL Quantum yields were measured using a Shimadzu RF-5301PC spectrofluorimeter (detector corrected) and Perkin Elmer Lambda 9 UV/VIS/NIR spectrophotometer using quinine sulfate dihydrate in 0.05 M H_2SO_4 as standard. UV/VIS absorption and photoluminescence

[a]*Institute of Chemistry and Technology of Organic Materials (ICTOS), Graz University of Technology, Stremayrgasse 16, A-8010, Graz, Austria. E-mail: slugovc@tugraz.at; Fax: +43316 873 8951; Tel: +43316 873 8454*
[b]*Institute of Solid State Physics, Graz University of Technology, Petersgasse 16, A-8010, Graz, Austria. E-mail: egbert.zojer@tugraz.at; Fax: +43316 873 8466; Tel: +43316 873 8475*
[c]*School of Chemistry and Biochemistry, Georgia Institute of Technology, 770 State Street, Atlanta, GA, 30332-0400, USA*

† Electronic supplementary information (ESI) available: details of synthesis, detailed absorption and fluorescence spectra of the introduced materials, details of computational methodology and CI description of the excited states. See DOI: 10.1039/b600912c

(PL) spectra were recorded in diluted solutions of $CHCl_3$–MeOH (1 : 1) at room temperature under ambient conditions. Fluorescence titrations and the evaluation of PL quantum yields of the protonated and/or deprotonated species were also performed in $CHCl_3$–MeOH (1 : 1) by adding diluted solutions of CF_3COOH or KO^{t}Bu. The refractive index of the solvent mixture $CHCl_3$–MeOH (1 : 1) was determined with an Abbe-Refractometer at 20 °C for the calculation of the PL quantum yield (n_D^{20} 1.388).

Synthesis

8-Benzyloxy-5,7-bis(biphenyl-4-yl)quinoline (4). Similarly to the procedure of Shoji *et al.*,[7] a suspension of **2** (100 mg, 0.254 mmol), biphenyl boronic acid (125 mg, 0.631 mmol) and Na_2CO_3 (300 mg, 2.830 mmol) in toluene (3 mL), EtOH (3 mL) and H_2O (3 mL) was degassed for 30 minutes. After adding $[Pd(PPh_3)_4]$ (25 mg, 0.022 mmol) the reaction mixture was heated for 24 hours at 95 °C under an inert argon atmosphere. Products were extracted with CH_2Cl_2, and dried over Na_2SO_4. The band with $R_f = 0.5$ (cy : ee = 3 : 1) was sampled in the course of column chromatography on silica using cy : ee = 10 : 1 as solvent giving **4** (120 mg, 87.4%) as a yellow solid. Anal. Calc. for $C_{40}H_{29}NO$: C, 89.02; H, 5.42; Found: C, 89.22; H, 5.29%. ν_{max}(film)/cm^{-1}: 3029m, 2925m, 1599m, 1519w, 1486s, 1453s, 1396m, 1370m, 1338s, 1214m, 1186m, 1164w, 1108w, 1075s, 1007s, 912s, 881w, 840s, 793m, 766s, 735s and 696s. δ_H(500 MHz, $CDCl_3$): 9.09 (1H, dd, $^3J_{HH}$ 3.9 and $^4J_{HH}$ 1.5, q^2), 8.40 (1H, dd, $^3J_{HH}$ 8.3 and $^4J_{HH}$ 1.5, q^4), 7.82–7.25 (25H, m, bn^{2,3,4,5,6}, 2 × bp$^{2,3,5,6,2',3',4'5',6'}$, q^3, q^6) and 5.29 (2H, s, CH_2); δ_C(125 MHz, $CDCl_3$): 151.4 (1C, q^8), 149.9 (1C, q^2), 143.8 (1C, q^{8a}), 141.0, 140.7, 140.6, 140.3, 138.3, 137.5, 137.2, 135.7, 133.7 (9C, q^{5,7}, 2 × bp$^{1,1',4}$, bn^1), 134.7 (1C, q^4), 130.7, 130.5, 129.0, 129.0, 128.7, 128.1, 127.8, 127.6, 127.5, 127.4, 127.3, 127.2, 127.0 (24C, bn^{2,3,4,5,6}, 2 × bp$^{2,3,5,6,2',3',4'5',6'}$, q^{4a}), 129.7 (1C, q^6), 121.3 (1C, q^3) and 76.7 (1C, CH_2).

5,7-Bis(dibenzothiophen-4-yl)-8-benzyloxyquinoline (5). A suspension of **2** (100 mg, 0.254 mmol), dibenzothiophene-4-boronic acid (139 mg, 0.609 mmol) and Na_2CO_3 (300 mg, 2.830 mmol) in toluene (3 mL), EtOH (3 mL) and H_2O (3 mL) was degassed for 30 minutes. After adding $[Pd(PPh_3)_4]$ (25 mg, 0.022 mmol) the reaction mixture was heated for 24 hours at 95 °C under an inert argon atmosphere. Products were extracted with CH_2Cl_2 and dried over Na_2SO_4. Sampling the band with $R_f = 0.5$ (cy : ee = 3 : 1) by column chromatography on silica with the solvent cy : ee = 7 : 1 yielded **5** (130 mg, 85.2%) as a yellow solid. Anal. Calc. for $C_{40}H_{25}NOS_2$: C, 80.10; H, 4.20; Found: C, 80.26; H, 4,13%. ν_{max}(film)/cm^{-1}: 3063m, 2925m, 1571m, 1497m, 1441s, 1385m, 1342m, 1322w, 1303w, 1249m, 1216m, 1169m, 1109m, 1076m, 1046m, 908s, 795m, 751s, 728s and 694s. δ_H(500 MHz, $CDCl_3$): 9.08 (1H, dd, $^3J_{HH}$ 3.9 and $^4J_{HH}$ 2.0, q^2), 8.26–8.19 (4H, m, 2 × th^{1,8}), 8.06 (1H, dd, $^3J_{HH}$ 8.3 and $^4J_{HH}$ 2.0, q^4), 7.93 (1H, s, q^6), 7.79–7.38 (11H, m, q^3, 2 × th^{2,3,5,6,7}), 7.07–7.03 (5H, m, bn^{2,3,4,5,6}) and 5.25 (2H, 2 × d, $^2J_{HH}$ 11.1,CH_2); δ_C(125 MHz, $CDCl_3$): 152.6 (1C, q^8), 150.1 (1C, q^2), 143.8 (1C, q^{8a}), 140.9, 140.1, 139.8, 137.3, 136.2, 136.0, 135.9, 135.8, 134.0, 133.9, 133.1, 132.8 (13C, q^{5,7}, bn^1, 2 × th$^{quart.\,C}$), 134.8 (1C, q^4), 129.5, 129.1, 128.7, 127.6, 127.1, 126.8, 124.9, 124.6, 124.4, 122.9, 122.8, 122.0, 121.8, 121.2, 120.9 (16C, bn^6, q^6, 2 × th1,^{2,3,5,6,7,8}), 128.3 (2C, bn^{3,5}), 128.0 (2C, bn^{2,6}), 127.8 (1C, q^{4a}), 121.7 (1C, q^3) and 77.0 (1C, CH_2).

General procedure for the preparation of 5,7-disubstituted 8-hydroxyquinoline derivatives (6–8)

Referring to a known procedure,[9] a suspension of the benzylated derivatives (**3–5**) and KI (15.9–25.8 eq.) in acetonitrile was carefully degassed. After adding $BF_3{\cdot}Et_2O$ (11.5–20.6 eq.) under an inert argon atmosphere, the reaction mixture was heated for 24 hours at 80 °C. Quenching with H_2O, adding aqueous $Na_2S_2O_3$ (10%, 4 mL) and aqueous HCl (10%, 2 mL) gave the crude products after extraction with CH_2Cl_2 and drying over Na_2SO_4. The products were purified by precipitation from hot methanol.

8-Hydroxy-5,7-diphenylquinoline (6). Compound **6** was obtained using **3** (160 mg, 0.413 mmol), KI (1.090 g, 6.566 mmol) and $BF_3{\cdot}Et_2O$ (0.6 mL, 4.7 mmol) in CH_3CN (20 mL) giving **6** (50 mg, 40.7%) as a yellow-brown solid. Compound **6** has been prepared from **3** before by Shoji and co-workers using Pd/C and cyclohexa-1,4-diene.[7]

5,7-Bis(biphen-4-yl)-8-hydroxyquinoline (7). Compound **7** was prepared starting from **4** (70 mg; 0.130 mmol) by adding KI (360 mg, 2.169 mmol) and $BF_3{\cdot}Et_2O$ (0.2 mL, 1.6 mmol) in CH_3CN (10 mL) yielding **7** (20.8 mg, 35.8%) in a yellow-brown solid form. Anal. Calc. for $C_{33}H_{23}NO$: C, 88.17; H, 5.16; Found: C, 88.25; H, 5.22%. ν_{max}(film)/cm^{-1}: 3327m, 3028m, 1600w, 1574m, 1520w, 1496s, 1487s, 1456s, 1408s, 1372m, 1325m, 1265m, 1180m, 1162m, 1108w, 1075w, 1007m, 941w, 907m, 841s, 792m, 765s, 733s and 696s. δ_H(500 MHz, $CDCl_3$): 9.44–8.69 (1H, bs, OH), 8.86 (1H, d, $^3J_{HH}$ 3.4, q^2), 8.40 (1H, d, $^3J_{HH}$ 8.3, q^4) and 7.97–7.37 (20H, m, q^3, q^6, 2 × bp$^{2,3,5,6,2',3',4',5',6'}$). δ_C(125 MHz, $CDCl_3$): 148.5 (1C, q^8), 148.1 (1C, q^2), 141.0, 140.8, 140.4, 140.2, 138.8, 138.4, 136.6 (7C, q^{8a,} 2 × bp$^{1,1',4}$), 134.8 (1C, q^4), 130.6, 129.9, 129.0, 128.9, 127.6, 127.4, 127.4, 127.3, 127.3, 127.3 (19C, q^6, 2 × bp$^{2,3,5,6,2',3',4',5',6'}$), 130.5, 126.0, 121.9 (q,$^{4^a,5,7}$) and 121.9 (1C, q^3).

5,7-Bis(dibenzothiophen-4-yl)-8-hydroxyquinoline (8). Compound **8** was obtained by the reaction of **5** (70 mg, 0.117 mmol) with KI (500 mg, 3.012 mmol) and $BF_3{\cdot}Et_2O$ (0.3 mL, 2.4 mmol) in CH_3CN (15 mL) giving **8** (30 mg, 50.4%) as a yellow-brown solid. Anal. Calc. for $C_{33}H_{19}NOS_2$: C, 77.77; H, 3.76; Found: C, 77.83; H, 3.69%. ν_{max}(film)/cm^{-1}: 3350m, 3063m, 1576m, 1499m, 1480m, 1460s, 1441s, 1416m, 1374m, 1334m, 1302m, 1261s, 1195m, 1170m, 1089m, 1045m, 906s, 817w, 793s, 750s, 728s, 691m and 600w; δ_H(500 MHz, $CDCl_3$): 9.30–8.60 (1H, bs, OH), 8.88 (1H, dd, $^3J_{HH}$ 3.9 and $^4J_{HH}$ 1.4, q^2), 8.25–8.19 (4H, m, 2 × th^{1,8}), 8.08 (1H, dd, $^3J_{HH}$ 8.3 and $^4J_{HH}$ 1.4 Hz, q^4), 8.00 (1H, s, q^6) and 7.82–7.41 (1H, m, q^3, 2 × th^{2,3,5,6,7}); δ_C(125 MHz, $CDCl_3$): 149.3 (1C, q^8), 148.4 (1C, q^2), 141.1 (1C, q^{8a}), 139.9, 139.8, 136.3, 136.2, 136.0, 135.9, 133.9, 132.5 (12C, q^{5,7}, 2 × th$^{quart.C}$), 135.1 (1C, q^4), 130.1, 128.8, 128.7, 127.1, 126.8, 125.0, 124.8, 124.6, 124.4, 122.9, 122.8, 122.2, 122.0, 121.8, 121.0, 121.0 (16C, q^{3,6}, 2 × th^{1,2,3,5,6,7,8}) and 126.3 (1C, q^{4a}).

Quantum-mechanical calculations

To provide microscopic insight into the electronic and optical properties of the investigated materials, we have calculated the optical properties of the investigated molecules using semi-empirical methods. Ground-state equilibrium geometries have been optimized at the AM1 level[10] using Ampac 6.55. Excitation energies and transition dipole moments have been calculated by

This journal is © The Royal Society of Chemistry 2006

coupling the INDO/S Hamiltonian[11] to a single configuration interaction (SCI) scheme as implemented by Zerner and co-workers. The size of the SCI active space is scaled with the number of π-electrons. To optimize excited state geometries (which is necessary to describe emission properties), the AM1-SCI technique as implemented in AMPAC has been used.[12] Details regarding the CI-active spaces can be found in the ESI†. In the studied model systems (**2**′, **3**′, **4**′, **5**′) the benzyloxy group of **2**, **3**, **4**, and **5** is replaced by a methoxy group.

For comparative reasons, we have also performed studies using time-dependent density functional theory (TD-DFT) on the basis of DFT optimized geometries at the B3LYP/6-31G(d,p) level using Gaussian98 Rev. A.11.[13] In the case of the non-protonated molecules, the obtained results are comparable to the semi-empirical ones although agreement with the experimental results is slightly worse. For the protonated systems, we, however, observe a less satisfactory performance of TD-DFT with the calculations in some cases, for example predicting excited states located more than 1 eV below the experimentally observed ones. This is in fact quite a general observation that we have made investigating a large number of different protonated/deprotonoted molecules with various types of conjugated backbones. The origin for that deviation is not yet fully understood but could be related to self interaction effects modified by the change of nuclear charge, although in that case the failure for cations appears somewhat surprising. To gain a full understanding of this rather technical aspect, further investigations will be necessary. In this context it also needs to be stressed that solvent related effects and the influence of counterions for the protonated molecules have been neglected in the present calculations.

Results and discussion

Synthesis

The synthetic pathway used to prepare compounds **2–8** is shown in Scheme 1.

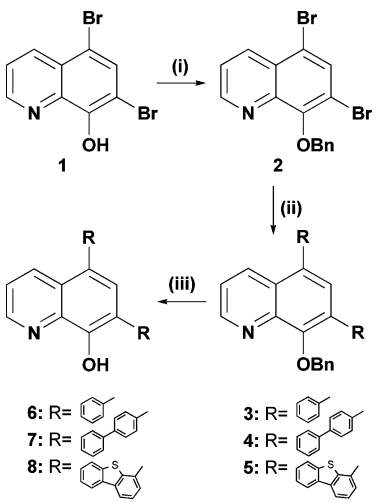

Scheme 1 Synthesis of 5,7-disubstituted-8-hydroxyquinoline derivatives: (i) benzyl bromide, KOH, EtOH, H_2O, 100 °C, 20 hours; (ii) boronic acid, $[Pd(PPh_3)_4]$, toluene, EtOH, H_2O, Ar, 95 °C, 24 hours; (iii) $BF_3{\cdot}Et_2O$, KI, CH_3CN, Ar, 80 °C, 24 hours. Bn = benzyl.

The benzyloxy-group was attached to 5,7-dibromo-8-hydroxyquinoline (**1**) by the reaction with benzyl bromide and KOH in EtOH–H_2O at 100 °C for 20 hours. After cooling to room temperature, the precipitate was filtered off, washed with cold methanol and purified by column chromatography on silica. To remove the by-product benzyl alcohol, the solid residue was washed with hot methanol several times yielding 8-benzyloxy-5,7-dibromoquinoline (**2**) as a white solid (43.4%). Following this pathway, two main goals could be achieved: (i) **2** is prone to be coupled *via* a palladium-catalysed Suzuki cross-coupling reaction with boronic acids, while **1** is not, due to deactivation of the catalytically active palladium-species by forming a palladium complex (presumably $[Pdq_2]$)[4] and (ii) the ESIPT is blocked by introduction of the protecting group.

8-Benzyloxy-5,7-diphenylquinoline (**3**), 8-benzyloxy-5,7-bis-(biphenyl-4-yl)quinoline (**4**) and 5,7-bis(dibenzothiophen-4-yl)-8-benzyloxyquinoline (**5**) were prepared under palladium-catalysed conditions by the cross-coupling of **2** with the corresponding boronic acids using the catalyst tetrakis(triphenylphospine)-palladium ($[Pd(PPh_3)_4]$) in a solvent mixture of toluene, EtOH and H_2O in the presence of Na_2CO_3. After refluxing for 24 hours at 95 °C under an inert argon atmosphere, the products could be isolated in pure form after column chromatography on silica in 30.4%, 87.4% and 85.2% yield. **3–5** were characterized by IR, ^{1}H- and ^{13}C-NMR spectroscopy as well as by elemental analysis.

The success of the Suzuki cross-coupling reaction preparing compounds **3–5** was strongly dependent on the catalyst used. Experiments to reduce the reaction time and to permit milder reaction conditions using the recently described, air-stable catalyst *trans*-bis(dicyclohexylamine)palladium-diacetate ($[trans\text{-}Pd(OAc)_2(NHCy_2)_2]$, "DAPCy")[14] gave rise to varying amounts of by-products which were identified as mono-substituted 8-benzyloxyquinoline derivatives (*c.f.* ESI†). Although these by-products could be easily identified in ^{1}H-NMR spectra, attempts to separate them from **3–5** using column chromatography on silica failed. However, these experiments showed that the ^{1}H-NMR signal of the benzyloxy-group can be used for the examination of the purity of the formed 8-benzyloxy-5,7-disubstituted quinoline derivatives. As depicted in Fig. 1, a mixture of mono- and disubstituted products results in two signals for the protons of the methylene group. While the protons of the OCH_2-group of **2**, **3** and **4** could be assigned to singlets at 5.47 ppm, 5.22 ppm and 5.29 ppm, the signal-form (two broadened doublets) of the now diasterotopic CH_2O-group of **5** at 5.25 ppm indicates a restricted rotation of the benzyloxy group (see Fig. 1). Another fact obtained from ^{1}H-NMR spectra is the different shift of the protons 2 and 4 of the quinoline core (q^2 and q^4) of mono- and disubstituted products. Even though the signals of q^2 and q^4 differ less than those of the methylene moiety, they can be used for a quick control of product-purity (see ESI†). Attempts to separate the mono-substituted products by column chromatography on silica for the preparation of asymmetrically substituted 8-benzyloxyquinoline derivatives failed because of similar R_f values. It is worth noting that beside the residual signal for *C*-Br no significant difference between mono- and disubstituted products can be noticed by ^{13}C-NMR spectroscopy.

For the preparation of 8-hydroxy-5,7-diphenylquinoline (**6**), 5,7-bis(biphen-4-yl)-8-hydroxyquinoline (**7**) and 5,7-bis(dibenzothiophen-4-yl)-8-hydroxyquinoline (**8**), the benzyloxy-group was

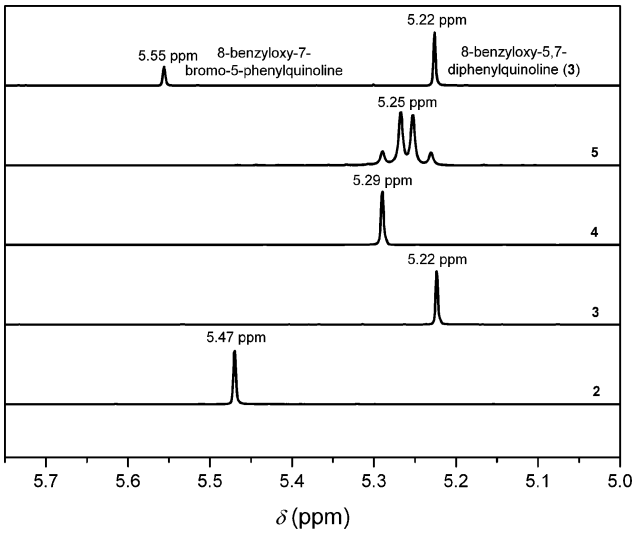

Fig. 1 ^{1}H-NMR signals of the benzyloxy-group of compounds **2–5**. Mono-coupling products can be identified by different shifts of the protecting group.

removed after activation with $BF_3 \cdot Et_2O$ by the nucleophilic attack of KI in acetonitrile. The dark coloured solutions (formation of iodine in the reaction) were treated with aqueous $Na_2S_2O_3$, acidified and purified by precipitation from methanol to remove the formed benzyl iodide. Compounds **6–8** could be isolated in analytically pure form in moderate yield (40.7% for **6**, 35.8% for **7** and 50.4% for **8**). The above described cleavage of the protecting group was chosen because we encountered difficulties when using conventional catalytic hydrogenolysis protocols.[7] In this case, the need for separation of unreacted **3**, **4** or **5** led, in our hands, to yields below 10%.[15]

Absorption spectra and quantum mechanical calculations

UV/VIS absorption was recorded in diluted solutions of $CHCl_3$–MeOH (1 : 1) at room temperature under ambient conditions. The optical data for the absorption of compounds **2–5** are summarised in Table 1, their absorption spectra are shown in Fig. 2. In the measured solutions all compounds exhibit a main absorption peak at 245 nm, 257 nm, 282 nm and 242 nm, respectively. At longer wavelengths, absorption peaks in the region of 308 nm, 320 nm and 334 nm can be detected for compounds **2–4**. For **5** two absorption peaks at 289 nm and 330 nm are observed.

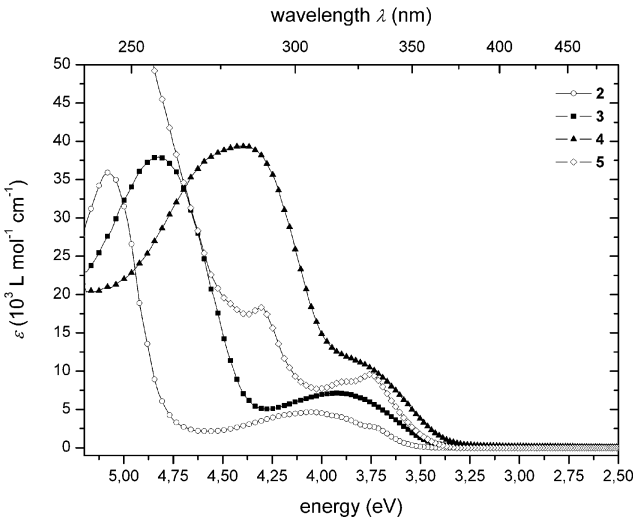

Fig. 2 Absorption spectra of compounds **2–5** in dilute $CHCl_3$–MeOH (1 : 1) solution.

The INDO-SCI calculated energies, wavelengths and oscillator strengths[16] for the first excited state as well as higher lying states with significant oscillator strengths are also listed in Table 1

Table 1 Experimentally obtained absorption maxima for **2**, **3**, **4** and **5** and INDO/SCI calculated excitation energies, wavelengths and oscillator strengths of the dominant one-photon states in molecules **2′**, **3′**, **4′**, and **5′**. (Details regarding the CI-description of the states can be found in the ESI†)

Molecule	E/λ (eV/nm)	ε (L mol^{-1} cm^{-1})	Molecule/state	E (eV)	OS
2			**2′**		
			S_1	3.96	0.00
	3.73/332	2800			
	4.05/308	4700	S_4	4.45	0.16
	5.28/245	36000	S_7	5.23	0.93
3			**3′**		
			S_1	3.74	0.00
	3.92/320	7100	S_2	3.95	0.22
	4.83/257	38000	S_6	4.65	1.37
			S_7	4.84	0.28
4			**4′**		
			S_1	3.72	0.01
	3.72/334	11000	S_2	3.89	0.38
	4.42/282	39000	S_4	4.26	1.15
	shoulder		S_6	4.30	0.78
	high energy tail		S_9	4.56	0.53
5			**5′**		
			S_1	3.75	0.00
	3.76/330	9600	S_2	4.00	0.15
	3.90/317	8500	S_4	4.08	0.12
	4.31/289	18000	S_8	4.49	1.43
			S_9	4.54	0.39
			S_{10}	4.62	0.72
	5.11/242	81000	S_{18}	5.33	0.50

This journal is © The Royal Society of Chemistry 2006

for model-molecules **2′**, **3′**, **4′**, and **5′**. A comparison with the measured data shows that the experimental observations are fully reproduced by the calculations. All molecules are characterized by a lowest lying state with vanishing oscillator strength (which is thus not visible in the experiments), a relatively weakly allowed state at smaller energies and a higher energy state with significantly increased oscillator strength. For the weak low-energy peak (which in the absorption spectrum of **4** is only visible as a shoulder) one observes a shift to lower energies (0.33 eV/0.38 eV in the measurements/calculations) with increasing conjugation length going from **2** to **3** to **4**. A much more pronounced shift is obtained for the strongest maximum at higher energies (between 4.25 eV and 5.0 eV) both in the calculations and in the measurements. To understand this behaviour, it is necessary to have a closer look at the actual electronic structure of the excited states and, as a first step, at the molecular orbitals involved in the excitation.

From the plots in Fig. 3 it becomes evident that the highest occupied molecular orbital (HOMO) and to an even greater extent the HOMO−1 in **4′** (as a representative example for this class of molecules) are delocalized over the molecular backbone and therefore strongly affected by increased conjugation due to the biphenyl substituents in positions 5 and 7. The lowest unoccupied molecular orbital (LUMO) is largely concentrated on the central hydroxyquinoline unit, while the LUMO+1 is again strongly delocalized. In all molecules, the first optically allowed state is largely described by an excitation from the HOMO to the LUMO while the HOMO−1 and LUMO+1 also strongly contribute to the description of the main maximum (details regarding the CI descriptions of the excited states can be found in the ESI†). This is fully consistent with the stronger conjugation length dependence of the latter peak.

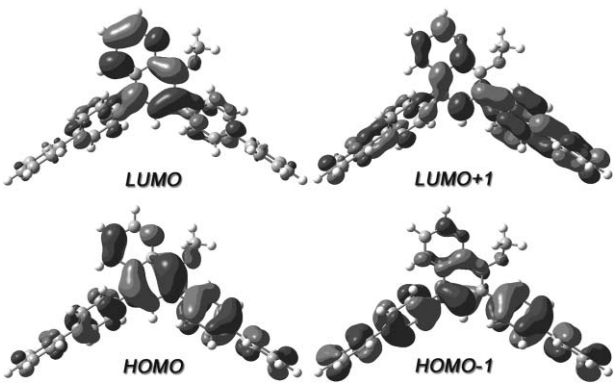

Fig. 3 INDO calculated highest occupied and lowest unoccupied molecular orbitals of **4′** (a coloured figure can be found in the ESI†).

The different nature of the various excited states becomes even more obvious from the electron-hole two particle wavefunctions in Fig. 4, which describe the correlated motion of the electron-hole pair. Here, the shading represents the probability of finding the hole at the site x, while the electron is at site y.[17] The S_1 state, which is optically forbidden, is strongly localized on the hydroxyquinoline unit. In the first allowed state S_2 especially, the hole is already somewhat delocalized and the state responsible for the main peak (S_4) is fully delocalized over the backbone with, in fact, higher probabilities for the electron and the hole to be at the substituents (especially that at the 5-position

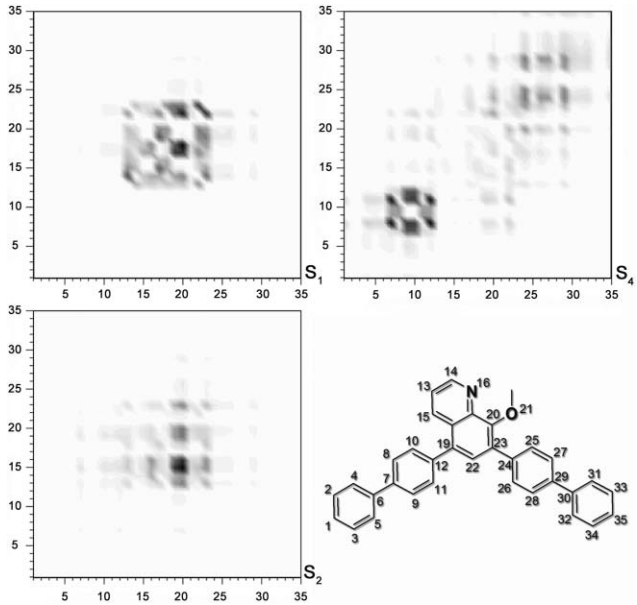

Fig. 4 INDO/SCI calculated e–h two-particle wavefunctions for the S_1 (top-left), S_2 (top-right), and S_4 (bottom-left) states of **4′**. The shading gives the probability of finding the hole on the site represented by the x-axis, while the electron is on the site given by the y-axis. The numbering of the sites is shown schematically in the bottom right corner.

of the hydroxyquinoline). This more pronounced delocalisation explains why the main maximum is most strongly affected by increasing the conjugation length.

Compound **5′** somewhat deviates from the general trends observed for the other three materials. There are several low-lying states, whose energies and oscillator strengths somewhat differ for different conformations. This can be explained by the observation that different orientations of the substituents result in different sterical constraints, thus different twist angles and, in turn, different degrees of electronic coupling between the quinoline core and the substituents in the 5 and 7 positions. The results contained in Table 1 have been obtained for the conformation shown in the ESI†. Also in the higher energy region the situation is clearly more complex than in the other materials with three states with oscillator strengths >0.3 around 4.5 eV and five states between 5.3 and 5.7 eV. The superposition of the associated peaks assuming a Gaussian broadening with a FWHM of 0.4 eV then yields two maxima at 4.52 eV and 5.64 eV, where the relative intensity of the lower energy maximum is clearly overestimated compared to the experiment.

Protonation of 2, 3, 4 and 5

To test the applicability of the presented materials as pH probes, we further investigated the photophysical properties of **2**, **3**, **4** and **5** upon addition of 10 μL conc. trifluoracetic acid (TFA). By doing so, we anticipated a protonation of all molecules at the quinoline nitrogen atom forming **2-H**$^+$, **3-H**$^+$, **4-H**$^+$ and **5-H**$^+$. From the resulting absorption and emission spectra (*vide infra*) it turned out that in the case of **2** almost no protonation occurred. Even upon addition of another 10 μL TFA conc. no significant change of the absorption spectrum was detected. In contrast, **3**, **4** and **5** were completely protonated under the conditions used, as indicated by

the formation of yellow coloured solutions and thus significantly altered absorption spectra (*c.f.* Fig. 5). Addition of another 10 μL of TFA resulted in no further changes. Absorption maxima for **3-H**$^+$, **4-H**$^+$ and **5-H**$^+$ are presented in Table 2. Again INDO/SCI calculations were performed in order to understand the observed changes in the absorption spectra.

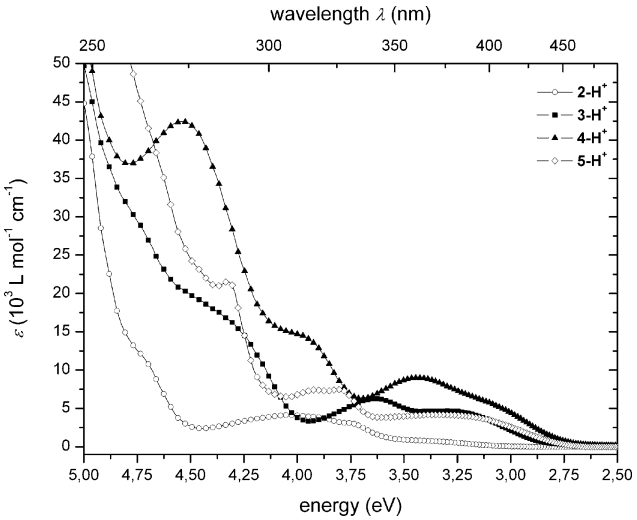

Fig. 5 Absorption spectra of compounds **2–5** in their protonated forms.

As far as the electronic states in the protonated molecules are concerned, the most intriguing aspect is the appearance of two optically allowed excited states below the first state of the non protonated systems, as consistently observed in the experiments (appearance of shoulders) and in the calculations. Concerning the quantitative agreement between theory and experiment, the INDO/SCI calculations here somewhat underestimate the energies of the excited states (*i.e.*, overestimate the shift resulting from the protonation) but otherwise give a realistic picture. We attribute this overestimation of the shift to the neglect of interactions with solvent and/or counterions in the calculations. Hydrogen bonding and the impact of solvents on the proton transfer has, for example, been described by Lehtonen *et al.*[18] for the methanesulfonic acid–pyridine complex. In the actual system such interactions should similarly weaken the bonding between the proton and the nitrogen in the hydroxyquinoline.

In **3′** the CI descriptions of the two low-lying states are dominated by excitations from the HOMO−1 and the HOMO into the LUMO. Here, the two occupied orbitals are delocalized over the whole molecule, while the LUMO is strongly localized on the central quinoline unit. The localisation is even more pronounced in **4′** where the HOMO and the HOMO−1 are each largely localized on one of the biphenyl substituents, while the LUMO is again localized on the quinoline (see orbital plots in the ESI†). Only the HOMO−4, which plays a role in the description of the S_1 state (see ESI), is delocalized over the whole backbone. This is consistent with the relatively low oscillator strength of these excited states as well as with the fact that in the exciton the hole is delocalized over the backbone, while the electron is strongly localized on the quinoline (see e–h plots in the ESI).

The UV/VIS spectra of **6**, **7** and **8** are similar to the spectra of **3**, **4** and **5** and are therefore not discussed here. Data can be found in the ESI†.

Table 2 Experimentally obtained absorption maxima for **2-H**$^+$, **3-H**$^+$, **4-H**$^+$, and **5-H**$^+$ and INDO/SCI calculated excitation energies, wavelengths and oscillator strengths of the dominant one-photon states in the protonated species **2′-H**$^+$, **3′-H**$^+$, **4′-H**$^+$, and **5′-H**$^+$. (Details regarding the CI-description of the states can be found in the ESI†)

Molecule	E/λ (eV/nm)	ε (L mol^{-1} cm^{-1})	Molecule/state	E (eV)	OS
2-H$^+$			**2′-H**$^+$		
	—[a]	—[a]	S_1	3.42	0.11
	—[a]	—[a]	S_4	4.70	0.82
3-H$^+$			**3′-H**$^+$		
	3.27/380	4800	S_1	2.84	0.18
	3.63/341	6400	S_2	3.35	0.26
			S_5	4.08	0.30
	4.46/278	19000	S_7	4.53	0.22
	4.46/278	19000	S_{11}	4.66	0.37
			S_{12}	5.06	0.22
4-H$^+$			**4′-H**$^+$		
			S_1	2.64	0.21
	3.08/402	5600	S_2	2.92	0.41
	3.44/360	9000	S_3	3.74	0.26
	3.99/311	15000	S_7	4.12	0.38
			S_8	4.24	0.39
	4.54/274	42000	S_{12}	4.44	0.49
			S_{19}	4.89	0.44
5-H$^+$			**5′-H**$^+$		
	3.21/386	4000	S_1	2.88	0.24
	3.80/326	7300	S_5	3.42	0.17
	3.92/316	7400	S_6	3.86	0.10
	4.33/286	21000	S_{10} [b]	4.17	0.42

[a] Almost no protonation occurred as indicated by a virtually unchanged absorption spectrum after addition of TFA. [b] Several states with intermediate oscillator strengths at higher energies.

This journal is © The Royal Society of Chemistry 2006

Table 3 Photoluminescence data of compounds **2–5** and **2-H⁺–5-H⁺**: Energies (E) and wavelengths (λ) of the luminescence maxima as well as luminescence quantum yields ($\varnothing_{PL}$) of the respective compounds. **2′–5′** and **2′-H⁺-5′-H⁺**: INDO/SCI calculated emission energies, wavelengths, oscillator strengths (OS) and radiative lifetimes (T_{rad}) for the lowest excited states of the model molecules as obtained for the S_1 excited state equilibrium geometries

Compound	E (eV)	λ (nm)	$\varnothing_{PL}$ (%)	OS	T_{rad}
2	3.16	393	<0.5	—	
2′	3.58	346	—	0.00	0.7 µs
2-H⁺	3.16[a]	393[a]	<0.5	—	
2′-H⁺	2.95	420	—	0.10	26.0 ns
3	2.91	426	14	—	
3′	3.37	368	—	0.35	5.8 ns
3-H⁺	2.41	515	9	—	
3′-H⁺	2.4	518	—	0.20	20.6 ns
4	2.88	430	16	—	
4′	3.24	383	—	0.80	2.7 ns
4-H⁺	2.28	545	12	—	
4′-H⁺	2.21	561	—	0.43	11.0 ns
5	2.95	421	2	—	
5-H⁺	2.12	584	1	—	

[a] No other emission was detected upon addition of CF_3COOH.

Photoluminescence

Photoluminescence (PL) spectra were obtained by excitation at 348 nm for all compounds. The peak energies of the resulting emission spectra of **2–5** are listed in Table 3 together with the measured PL quantum yields. In the non-protonated form, all molecules emitted in the blue spectral region (with maxima at 393 nm, 426 nm, 430 nm and 421 nm). With the exception of **2**, all compounds emitted at longer wavelengths after protonation with 10 µL TFA conc. (about 515 nm, 545 nm and 584 nm). Among these materials, **3** and **4** exhibited comparably good fluorescence intensities as indicated by quantum yields well above 10% ($\varnothing_{PL} = 14$ to 16%), while **2** and **5** showed poor fluorescence intensities with quantum yields below 2%. Similar behaviour was observed for the protonated species, albeit quantum yields are generally lower than in the unprotonated state. The results are best described by the fluorescence titrations depicted in Figs. 6 and 7. Dilute solutions of TFA in $CHCl_3$–MeOH (1 : 1) were added in microlitre quantities in the course of fluorescence titration experiments. The original emission was recovered in each case upon addition of KO^{t}Bu to the acidified solutions indicating the reversibility of the reaction.[19]

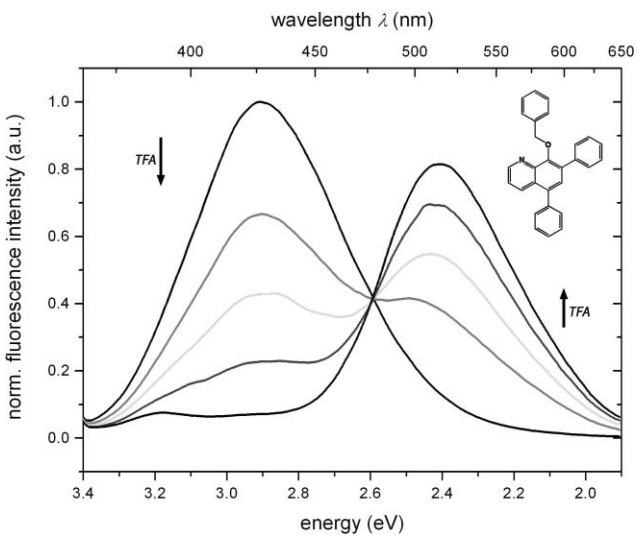

Fig. 6 Fluorescence titration of **3** with CF_3COOH ($\lambda_{Ex} = 348$ nm).

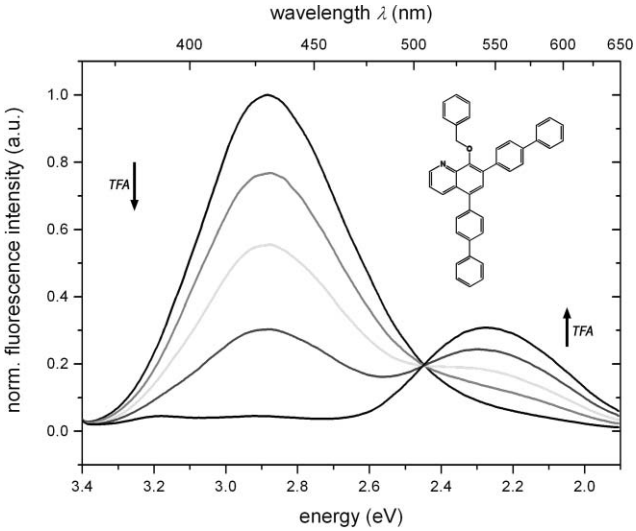

Fig. 7 Fluorescence titration of **4** with CF_3COOH ($\lambda_{Ex} = 348$ nm).

Compounds **1** and **6–8** as well as their protonated or deprotonated forms exhibited quantum yields below 1% rendering these materials unsuitable as fluorescent pH-probes. Corresponding data are gathered in the ESI†.

Again semi-empirical calculations were performed to rationalize the emission behaviour of **2–5**. The emission properties are determined by the characteristics of the lowest excited states at their equilibrium geometries. The energies and oscillator strengths of these states for the non protonated as well as for the protonated molecules are shown in Table 3. In **3′** and **4′** the order of the excited states changes compared to the results obtained for the ground-state equilibrium geometries (*c.f.* Table 3) rendering the lowest excited state optically allowed and the molecule emissive.[20] The Stokes shift is, however, somewhat underestimated by the calculations. In **2′** the optically forbidden state remains lowest in energy, which results in **2** being non fluorescent as observed in the experiment. This is a consequence of S_1 being a $\pi \rightarrow \sigma^*$ excited state, where the LUMO is a σ^* orbital localized at the C–Br bonds. For **5**, no conclusive answers for the emission properties have been obtained in the calculations, as here we find a large number of local minima of the S_1 geometry. The resulting transition energies differ by more than 1 eV (yielding in some cases transition energies clearly below the experimental observations) depending on the corresponding twist angle of the 2-dibenzothiophene substituents. For the lowest energy conformers found in our studies, interactions of the sulfur with hydrogen atoms in either position 4 or 6 of the quinoline moiety were detected.

In the protonated state, the calculations predict all molecules to be emissive, although with smaller 'oscillator strength' than in the non protonated state. In this context it has to be kept in mind that the oscillator strength is proportional to the energy of the excited state times the square of the transition dipole to the ground state; this is a direct measure for the 'absorption strength' of a

state. In contrast to that, spontaneous emission probabilities are proportional to the cube of the transition energy times the square of the transition dipole. Therefore, calculated radiative lifetimes[21] have also been included in Table 3.

The observed luminescence quantum yields in Table 3 as well as the emission spectra in Figs. 6 and 7 with the strongly shifted emission spectrum in the protonated species are thus at least qualitatively consistent with the measurements (for a quantitative comparison, a rigorous treatment of non-radiative deexcitation channels together with their pH dependence would be necessary).

Interestingly, we find that for both the protonated and non protonated forms of **3′** and **4′**, the coupling between the hydroxyquinoline core and the substituent at the 5 position is increased in the S_1 equilibrium geometry compared to the ground state. This can be concluded from both a reduction of the twist angle between the plane of the 5-substituent and the hydroxyquinoline (from 60° to 33° in **4′** and from 58° to 33° in **4′-H⁺**) and the corresponding e–h two-particle wavefunctions. In both molecules and both protonation states, the lowest lying optically allowed states are clearly more delocalized between the hydroxyquinoline and the substituent in the 5 position for the S_1 equilibrium geometry (for the case of molecule **4′** see ESI†). A similar effect was described in the literature on the basis of absorption measurements of Ru(COD)(hydroxyquinoline) complexes featuring differently substituted hydroxyquinolines.[22]

Conclusions

In summary, a series of 5,7-disubstituted 8-benzyloxyquinoline derivatives has been prepared by a Suzuki cross-coupling reaction. Photophysical measurements revealed adequate fluorescence properties due to an inhibited excited-state intramolecular proton transfer (ESIPT). For these compounds, modulation of the emission properties upon an external input (pH) could be detected, which opens up a possible application as ratiometric fluorescent pH-probes. The photophysical properties were rationalized by semi-empirical INDO/SCI calculations. Additionally the corresponding series of 5,7-disubstituted-8-hydroxyquinoline derivatives was synthesized. Albeit these materials alter their emission properties upon protonation and deprotonation, they suffer from the drawback of very low photoluminescence quantum yields which impede their use in pH sensing applications. Nevertheless, the synthesized π-extended 8-hydroxyquinoline derivatives have found,[5,7] and will find, use in electroactive or electroemissive materials as ligands for, *e.g.*, aluminium, zinc or boron. Efforts along these lines are currently underway in our laboratories.

Acknowledgements

Financial support by the Spezialforschungsbereich (SFB) Electroactive Materials of the Austrian Science Found FWF (project numbers F903 and F917) and the Austrian Nano Initiative (Research Project Cluster 0700-Integrated Organic Sensor and Optoelectronics Technologies-Research Project 0701 and 0702) is gratefully acknowledged. The work at Georgia Tech has been partly supported by the National Science Foundation (CRIF 04-43564). The authors would like to thank Filipp Furche and Jean-Luc Brédas for stimulating discussions.

References and notes

1 (*a*) J. I. Peterson and G. G. Vurek, *Science*, 1984, **224**, 123; (*b*) *Principles of Fluorescence Spectroscopy*, J. R. Lakowicz, Kluwer Academic/Plenum Publishers, New York, 1999; (*c*) *Molecular Switches*, B. L. Feringa, Wiley-VCH, Weinheim, 2001; (*d*) Z. Wang, G. Zheng and P. Lu, *Org. Lett.*, 2005, **7**, 3669.

2 (*a*) H. Ihmels, A. Meiswinkel and C. J. Mohrschladt, *Org. Lett.*, 2000, **2**, 2865; (*b*) J.-H. Liao, C.-T. Chen, H.-C. Chou, C.-C. Cheng, P.-T. Chou, J.-M. Fang, Z. Slanina and T. J. Chow, *Org. Lett.*, 2002, **4**, 3107; (*c*) J.-S. Yang, C.-S. Lin and C.-Y. Hwang, *Org. Lett.*, 2001, **3**, 889; (*d*) T. H. Kim and T. M. Swager, *Angew. Chem., Int. Ed.*, 2003, **42**, 4803; (*e*) J. V. Mello and N. S. Finney, *Angew. Chem., Int. Ed.*, 2001, **40**, 1536; (*f*) L. Fabrizzi, M. Licchelli, N. Marcotte, F. Stomeo and A. Taglietti, *Supramol. Chem.*, 2002, **14**, 127; (*g*) B. Liu and H. Tian, *Chem. Commun.*, 2005, 3156.

3 (*a*) M. D. Shults and B. Imperiali, *J. Am. Chem. Soc.*, 2003, **125**, 14248; (*b*) M. D. Shults, D. A. Pearce and B. Imperiali, *J. Am. Chem. Soc.*, 2003, **125**, 10591; (*c*) D. A. Pearce, N. Jotterand, I. S. Carrico and B. Imperiali, *J. Am. Chem. Soc.*, 2001, **123**, 5160; (*d*) N. Jotterand, D. A. Pearce and B. Imperiali, *J. Org. Chem.*, 2001, **66**, 3224; (*e*) R. T. Bronson, M. Montalti, L. Prodi, N. Zaccheroni, R. D. Lamb, N. K. Dalley, R. M. Izatt, J. S. Bradshaw and P. B. Savage, *Tetrahedron*, 2004, **60**, 11139; (*f*) R. T. Bronson, J. S. Bradshaw, P. B. Savage, S. Fuangswasdi, S. C. Lee, K. E. Krakowiak and R. M. Izatt, *J. Org. Chem.*, 2001, **66**, 4752; (*g*) L. Prodi, M. Montalti, N. Zaccheroni, J. S. Bradshaw, R. M. Izatt and P. B. Savage, *Tetrahedron Lett.*, 2001, **42**, 2941; (*h*) L. Prodi, C. Bargossi, M. Montalti, N. Zaccheroni, N. Su, J. S. Bradshaw, R. M. Izatt and P. M. Savage, *J. Am. Chem. Soc.*, 2000, **122**, 6769; (*i*) R. T. Bronson, D. J. Michaelis, R. D. Lamb, G. A. Husseini, P. B. Fransworth, M. R. Linford, R. M. Izatt, J. S. Bradshaw and J. B. Savage, *Org. Lett.*, 2005, **7**, 1105; (*j*) F. Launay, V. Alain, E. Destandau, N. Ramos, E. Bardez, P. Baret and J.-L. Pierre, *New J. Chem.*, 2001, **25**, 1269; (*k*) J. K. Winkler, C. M. Bowen and V. Michelet, *J. Am. Chem. Soc.*, 1998, **120**, 3237; (*l*) S. Y. Moon, N. R. Cha, Y. H. Kim and S. K. Chang, *J. Org. Chem.*, 2004, **69**, 181; (*m*) Y.-H. Kim, J. S. Youk, S. Y. Moon, J.-I. Choe and S.-K. Chang, *Chem. Lett.*, 2004, **33**, 702; (*n*) H. Zhang, L.-F. Han, K. A. Zachariasse and Y.-B. Jiang, *Org. Lett.*, 2005, **7**, 4217.

4 R. Ballardini, G. Varani, M. T. Indelli and F. Scandola, *Inorg. Chem.*, 1986, **25**, 3858.

5 For examples: (*a*) C. W. Tang and S. A. VanSlyke, *Appl. Phys. Lett.*, 1987, **51**, 913; (*b*) C. H. Chen and J. Shi, *Coord. Chem. Rev.*, 1998, **171**, 161; (*c*) V. A. Montes, G. Li, R. Pohl, J. Shinar and P. Anzenbacher, *Adv. Mater.*, 2004, **16**, 2001; (*d*) R. Pohl, V. A. Montes, J. Shinar and P. Anzenbacher, *J. Org. Chem.*, 2004, **69**, 1723; (*e*) Q. Wu, M. Esteghamatian, N.-X. Hu, Z. Popovic, G. Enright, Y. Tao, M. D'Iorio and S. Wang, *Chem. Mater.*, 2000, **12**, 79; (*f*) H. Jang, L.-M. Do, Y. Kim, T. Zyung and Y. Do, *Synth. Met.*, 2001, **121**, 1667.

6 E. Bardez, I. Devol, B. Larrey and B. Valeur, *J. Phys. Chem. B*, 1997, **101**, 7786.

7 E. Shoji, K. Miyatake, A. R. Hlil, A. S. Hay, T. Maindron, V. Jousseaume and J. P. Dodelet, *J. Polym. Sci., Part A: Polym. Chem.*, 2003, **41**, 3006.

8 H. E. Gottlieb, V. Kotylar and A. Nudelman, *J. Org. Chem.*, 1997, **62**, 7512.

9 Y. D. Vankar and C. T. Rao, *J. Chem. Res. (S)*, 1985, 232.

10 M. J. S. Dewar, E. G. Zoebisch, E. F. Healy and J. J. P. Stewart, *J. Am. Chem. Soc.*, 1985, **107**, 3902.

11 J. A. Pople, D. L. Beveridge and P. A. Dobosh, *J. Chem. Phys.*, 1967, **47**, 2026; J. Ridley and M. Zerner, *Theor. Chim. Acta*, 1973, **32**, 111.

12 *Ampac 5.0 User's Manual*, ©, 1994, Semichem, 7128 Summit, Shwanee, KS 66216.

13 M. J. Frisch, G. W. Trucks, H. B. Schlegel, G. E. Scuseria, M. A. Robb, J. R. Cheeseman, V. G. Zakrzewski, J. A. Montgomery, Jr., R. E. Stratmann, J. C. Burant, S. Dapprich, J. M. Millam, A. D. Daniels, K. N. Kudin, M. C. Strain, O. Farkas, J. Tomasi, V. Barone, M. Cossi, R. Cammi, B. Mennucci, C. Pomelli, C. Adamo, S. Clifford, J. Ochterski, G. A. Petersson, P. Y. Ayala, Q. Cui, K. Morokuma, P. Salvador, J. J. Dannenberg, D. K. Malick, A. D. Rabuck, K. Raghavachari, J. B. Foresman, J. Cioslowski, J. V. Ortiz, A. G. Baboul, B. B. Stefanov, G. Liu, A. Liashenko, P. Piskorz, I. Komaromi, R. Gomperts, R. L. Martin, D. J. Fox, T. Keith, M. A. Al-Laham,

 This journal is © The Royal Society of Chemistry 2006

C. Y. Peng, A. Nanayakkara, M. Challacombe, P. M. W. Gill, B. G. Johnson, W. Chen, M. W. Wong, J. L. Andres, C. Gonzalez, M. Head-Gordon, E. S. Replogle and J. A. Pople, *GAUSSIAN 98 (Revision A.11)*, Gaussian, Inc., Pittsburgh, PA, 2001.
14 B. Tao and D. W. Boykin, *J. Org. Chem.*, 2004, **69**, 4330.
15 Attempts to purify compounds **6–8** by column chromatography failed because of presumably complex formation of the products with metal ions contained in silica.
16 The convention used for the CI coefficients assumes that each configuration abbreviated, *e.g.*, by H→L is a normalized singlet wavefunction.
17 Here we follow the definition given in: L. Romaner, G. Heimel, H. Wiesenhofer, P. Scandiucci de Freitas, U. Scherf, J. L. Brédas, E. Zojer and WE. J. List, *Chem. Mater.*, 2004, **16**, 4667, rather than applying the symmetrized version we used in previous works.
18 O. Lehtonen, J. Hartikainen, K. Rissanen, O. Ikkala and L.-O. Pietila, *J. Chem. Phys.*, 2002, **116**, 2417.
19 *Molecular Fluorescence*, B. Valeur, Wiley-VCH, Weinheim, 2001.
20 In **3′** the splitting between the optically allowed and the lowest forbidden state is actually considerably smaller resulting in a different order for one of the tested CI spaces- see also ESI†.
21 For details regarding the calculations of the lifetimes see, *e.g.*, U. Rant, U. Scherf, M. Rehahn, P. Galda, J. L. Brédas and E. Zojer, *Synth. Met.*, 2002, **127**, 241.
22 C. Slugovc, A. Koppitz, A. Pogantsch and F. Stelzer, *Inorg. Chim. Acta*, 2005, **358**, 2718.